University of North Carolina Asheville
Journal of Undergraduate Research
Asheville, North Carolina
May 2022

Structural and Dynamic Analysis of Subunit *a* in *E. coli* F_1F_o ATP Synthase

Owen Dowdall
Department of Chemistry & Biochemistry
The University of North Carolina Asheville
One University Heights
Asheville, North Carolina 28804 USA

Faculty Advisor: Dr. Ryan Steed

Abstract

ATP synthase is a membrane embedded protein that is ubiquitous among all forms of life. ATP synthase is the primary site of ATP production, which makes this protein crucial for many biological processes. ATP synthase is divided into two coupled motors denoted F_1 and F_o. F_1 is water soluble and contains the active site where ATP synthesis and hydrolysis occur through conformational changes. F_o is the membrane-embedded motor composed of a c-10-ring and ab 2 subunits, that drives the conformational changes in F_1 via a rotary mechanism in which protons flow down a potential gradient through two aqueous half channels in subunit a. Although there is considerable biochemical understanding of the mechanisms that occur in F_1, the processes that facilitate proton translocation in F_o are still not well understood. Structures of subunit a determined by cryo-electron microscopy (cryo-EM) reveals inconsistences in conformations of this subunit when compared to previous crosslinking studies. This inconsistency suggests that multiple conformational states are taken on by subunit a which could provide insight to the mechanism of proton translocation. While detergent solubilization methods prove effective for purifying ATP synthase, they do not account for any protein-membrane interactions that may occur. We instead are developing a SMALPs (styrene-maleic acid lipid particle) technique to extract ATP synthase into lipid nano discs allowing the protein to be studied in its native lipid environment. In nanodiscs, protein dynamics can be probed by electron paramagnetic resonance (EPR) spectroscopy, and compared to that of soluble protein in order to determine more precisely the effect the membrane has on the protein mechanism. Small scale extractions have been performed with several different SMALPs to varying degrees of efficiency, but large-scale extractions still prove unsuccessful. Successful EPR data could help shed light on the involvement of lipids in the F_o mechanism of ATP synthase.

1. Introduction

1.1. ATP Synthase

Research in biochemistry is fundamental to understanding the chemical processes that occur within living organisms. Many of these processes are facilitated by proteins and are crucial for maintaining homeostasis. Diseases are the result of malfunctions in these processes and medications are designed to target various protein functions. A firm understanding of biochemical mechanisms is critical for the continued treatment of ailments. ATP synthase (Figure 1) is a protein that is responsible for the synthesis and hydrolysis of adenosine triphosphate (ATP)[1] a molecule that provides the energy required for most biological processes. Effective ATP production is essential and ubiquitous; some form of ATP synthase (ATPase) is found in all forms of life.[2] Due to its abundance in biology, the mechanism of ATP synthase is thought to be one of the earliest developments in living organisms.[2] This protein bridges the phospholipid bilayer where it generates rotation *via* the passage of protons (H^+) from an area of higher concentration to an area of lower concentration. This rotation drives the conformational changes that facilitate the production of ATP which occurs in the intracellular half of the protein (denoted F_1). The membrane embedded segment (denoted

F_o) generates the rotation by converting the potential energy of the electrochemical gradient, created from the Electron Transport Chain (ETC), into mechanical energy which drives the conformational dynamics in F_1.

The F_1 segment consists of a αβ hexamer, the axle (γ and ε) and the peripheral stock (δ and *b*). F_o contains the rotor, which has 8-15 *c* subunits, and a subunit-*a* which is attached to F_1 by the peripheral stock (the stator).[1] The number of *c*-subunits varies among species (*c*-10 in *E. coli*).[1] ATPase is also known to work in reverse; by hydrolyzing ATP to ADP and P_i to pump H^+ to restore the electrochemical gradient.[3] Even though the function of ATPase is crucial and well known, the specific biophysical mechanism driving the rotation of the *c*-ring in F_o is unknown, as are any differences between the mechanisms of H^+ movement during ATP synthesis and hydrolysis. Since F_o is not water-soluble, high-resolution dynamics are difficult to discern. Gaining a better understanding of how the electrochemical potential energy is converted into mechanical rotation by F_o is crucial for understanding ATPase, and there are many implications for gaining insight into this process. These include the inhibition of bacterial ATPases by antibiotics, the development of treatments for mitochondrial related diseases and adding to the universal understanding of biological processes.

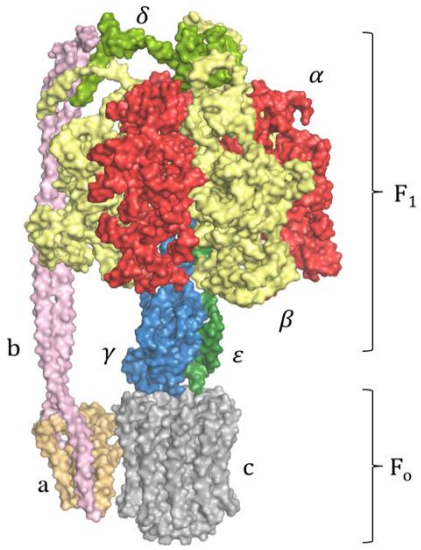

Figure 1: *E.coli* F-type ATPase with subunits labeled. PDB 5t4o

1.2. Review and Synthesis of Background Literature

ATP synthase is the primary source of ATP generation within organisms, but the mechanism behind the rotation that facilitates ATP synthesis is not yet understood. It was only in the late 1990s that the motion in F-type ATPase was confirmed by Hiroyuki *et al* through the use of actin filaments as fluorescent tags.[4] These studies additionally focused on the load bearing capacities of these actin filaments, and the torque generated was determined to be greater than 40 pN nm^{-1}. This confirmation raised more questions about how this rotation was generated, and prompted more studies focused on ATPase. Determining how proton translocation generates rotation involves probing the *c*-ring and the transmembrane helices (TMHs) of the *a*-subunit. Since the stator is the only structure stabilizing F_1F_o it suggests that the site of proton translocation is at the *ac*-interface. It then becomes necessary to probe the environment to determine if there are any conformational shifts and which amino acids may be important for those shifts.

In 2009, Steed *et al* published research supporting aqueous channels in the TMHs of subunit *a*,[5] whereby H^+ is given access to the intermembrane space and Asp61 *via* a hydrophilic channel. Steed *et al* probed the *ac*-interface by using Cys substitutions and testing Ag^+ and Cd^{2+} sensitivity. Later publications by Fillingame *et al* proposed two aqueous half-channels where H^+ enters through an aqueous channel at the periplasm side of *a*, where it is moved from *a*Arg210 (*E. coli*) to *c*Asp61 *via* a conformational change in *a* and exits through the cytoplasm side by the 36° ratcheting of the rotor.[2] This ultimately led to the mapping of the *a*-subunit and key residues expected to be involved in conformational shifts. In 2016 Sobti *et al* conducted several structural studies of ATP synthase using Cryo-EM and determined that

the 5 *a*TMHs present in *E. coli* were not perpendicular to the membrane as initially predicted.[1] The helices were almost horizontal, tilting ≈ 20° from the plane of the membrane. This change in orientation of the *a*TMHs is consistent with the aqueous half channels proposed by Fillingame *et al* as the conserved Arg210 does not differ in position from the vertical helix model. Sobti *et al* also proposed an ATP regulated conformational change in the *ε*-subunit that inhibits the rotation of F_1 thereby effectively regulating ATPase.

More recent structural studies have revealed the presence of cardiolipin (CD) packed around the *a* and *c* subunits. Muhleip *et al* obtained a Cryo-EM structure of *Euglena gracilis* dimeric ATP synthase with a resolution of 2.8 Å where bound CD could be identified.[6] Spikes *et al* had similar finding in bovine ATP synthase, where CD was bound about the aqueous channels.[7] In 2020 Sobti provided Cryo-EM structures with confirmed presence of lipids including cardiolipin and additionally found evidence that WT *E.coli* membranes were co-purified with their ATP Synthase.[8] Both Spikes and Muhleip suggest that CD could play a role in the dynamics and Spikes suggests that they could act as a gasket minimizing the leakage from the aqueous channels.[7,8] Han *et al* used a combination of EPR and reconstitution to compare the effects of the membrane on the electrostatic environment of the Proteorhodopsin binding site.[9] Reconstitution is a crucial method for determining dynamics of membrane imbedded proteins. LiGuo *et al* classified different reconstitution procedures as well as effects of detergents in the formation of proteolipids.[10]

Many computational studies have endeavored to provide biophysical models for torque generation in ATP synthase. The methods vary from stochastic approaches to electrostatics and energetics all of which reveal different information about the potential mechanism. Miller *et al* uses a combination of electrostatics and stochastic differentials equations in a model that treats the aqueous half channels as a dipole. Brownian motion is accounted for by the application of the Langevin equation to a particle in a washboard potential. This model results in highly nonlinear behavior of the system and suggests that a critical driving force (proton motive force or pmf in this case) is required to activate F_1.[11] Xin *et al* implemented the Fokker-Plank equation as well as Markov processes to synthesize a state dependent model based on the Brownian ratchet notion for molecular motors. This model provides a probabilistic description of the dynamics.[12] Kubo *et al* developed a dynamic model based on a molecular dynamics simulation coupled with a Monte Carlo simulation to identify the probabilities of all the dynamic states. The Monte Carlo method provides insight on probabilistic nature of the dynamics and serves as a framework for possible mechanical models.[13] These computational models provide information about dynamics that can otherwise be difficult to obtain by structural methods.

Site directed spin labeling (SDSL) has emerged as a novel technique for probing TMHs and determining the aqueous accessibility of the environment.[14] Altenbach *et al* used SDSL and electron paramagnetic resonance (EPR) to determine emersion of labels within bacteriorhodopsin, another intermembrane protein. EPR provides data that allows the label's environment to be parameterized computationally. In 1994 Zhang *et al* determined *via* site-directed mutagenesis that Asp61 (*E. coli*) on the *c*-subunit was highly conserved and thus must play a crucial role in H^+ translocation.[15] Further applications of EPR emerged when Hubbell *et al* explored the use of *S*-(1-oxyl-2,2,5,5-tetramethylpyrroline-3-methyl) methanethiosulfonate (MTSL) as a spin label and what governs its parameters, specifically distance to other labels, solvent accessibility, mobility, coupling with other paramagnetic centers and polarity.[16] Utilizing these parameters, Hubbell was able to determine secondary and tertiary structure variations and conformational dynamics on a number of transmembrane-proteins including rhodopsin and TonB.

Research conducted in Steed's lab consists of probing specific residues at the *ac*-interface expected to be involved in proton pumping. This is done using site-directed mutagenesis, as well as the determination of the involvement of residues within subunit-*a* in conformational changes *via* SDSL and EPR. Viability of mutants is tested using a proton pumping assay where ATPase containing inverted vesicles are combined with ATP and 9-amino-6-chloro-2-methoxyacridine (ACMA). If ATP is hydrolyzed, protons will be pumped into the vesicle which lowers the internal pH and protonates (quenches) ACMA which then becomes trapped in the vesicle. The protonation of ACMA causes it to lose aromaticity and thus it loses fluorescence. Proton pumping efficiency can then be determined by a fluorescence versus time graph, where wildtype is shown to have a decrease in fluorescence due to its quenching, and mutants with varying functionalities in proton pumping are shown to have varying fluorescence. ACMA is then removed from the vesicle by the addition of nigericin. A H^+ permeability assay also utilizes ACMA, and protons generated from the ETC.

Researching the conformational dynamics in subunit-*a* utilizes SDSL with MTSL and EPR to indicate any changes that could be occurring. These MTSL labels are reacted with His-tagged *E. coli* mutants and purified utilizing size exclusion chromatography. Previously, positions 93, 86, 179 and 195 were tagged and data on solvent accessibility, label mobility, and dipolar coupling were collected using EPR. Variations of distances between spin labels, as well as mobility, indicated conformational changes occurring at those positions or nearby positions. Data from previous work in this lab suggest several other residues on the cytoplasm half of subunit-*a* that have potential involvement in conformational changes.

The aM93C mutant is examined in detail with the intention of classifying its local environment *via* EPR. The primary goal of the project has been the development of a procedure for reconstitution. Reconstitution has been attempted in phosphatidylcholine with the intention of collecting EPR data from SL proteolipids in order to examine the effect of the membrane on functionality of both WT and mutant ATP synthase. The impact of the membrane on functionality as well as structure can be verified with functional assays and EPR. Development of a mathematical model of the system is also in progress in hopes that it will forecast some structural necessities for torque generation. Continuum electrostatic models utilizing the Poisson-Boltzmann Equation (PBE) offer overall visualizations of the surface potential in which the impact of point mutations on electrostatics can be observed. Since electrostatic models very quickly result in nonlinear partial differential equations (PDEs), a mechanical model is in development with the hopes of providing equations of motion for the dynamics of ATP synthase.

2. Experimental Methods

2.1. Purification

Purification of ATPase begins with growing of DK8: Δunc *E. coli* cultures in an LB medium (1:1:0.5, NaCl, Tryptone, Yeast extract). Small cultures are inoculated by adding frozen glycerol stock to 5mL of sterile LB and allowed to grow for 17-18 hours at 37℃. Additionally, 1L of LB is sterilized in triplicate in Fernbach flasks and inoculated with fresh small cultures. The 3L of large cultures are grown for 8 hours at 37℃ before the cells are pelleted for 15 minutes at 4000 xg. The cell pellets are then resuspended in TMDG buffer (TMG buffer, 1mM DTT *final*, 1mM pmsf *final*) where TMG is (50 mM Tris-HCl, 5 mM $MgCl_2$, 10% v/v glycerol, pH 7.5) by vortexing. The cell suspensions are then lysed through the homogenizer at ≥ 15,000 psi for 3 passes. The lysate is then spun at 9000 xg and the pellet is discarded. The remaining suspension is spun at 193,000 xg in the ultracentrifuge for 1 hour before the supernatant is decanted. The pellets are resuspended in ~10 mL of extraction buffer (20 mM Tris, 300 mM NaCl, 100 mM sucrose, 2 mM $MgCl_2$, 20 mM DTT, 20 mM imidazole, 1% DDM, 10% glycerol, pH 8.0) using a dounce, and allowed to rock for ≥ 1 hour at 4℃. This protein suspension is pelleted again at 100,000 rpm for 30 minutes in the ultracentrifuge. Care is taken when decanting the supernatant to avoid collecting any of the pellet, which is then discarded.

The protein is separated from the suspension using affinity chromatography with Thermo scientific HisPur Ni-NTA Resin beads. These are equilibrated by washing the beads with DI water by centrifugation and suspending them in ~10 mL of wash buffer (20 mM Tris, 300 mM NaCl, 100 mM sucrose, 2 mM $MgCl_2$, 20 mM imidazole, 0.05% DDM, 10% glycerol, pH 8.0) and allowing them to rock at 4℃. The beads are pelleted again, and the wash buffer is decanted before the protein suspension is added. The protein and the beads are allowed to rock for ≥60 minutes at 4℃. The solution is poured into a column and binding flow-through is collected. A column volume of wash buffer is added and the wash flow-through is collected. Next the elution buffer (20 mM Tris, 300 mM NaCl, 100 mM sucrose, 2 mM $MgCl_2$, 200 mM imidazole, 0.05% DDM, 10% glycerol, pH 8.0) is added and the elute is collected in 10-12 0.5 mL

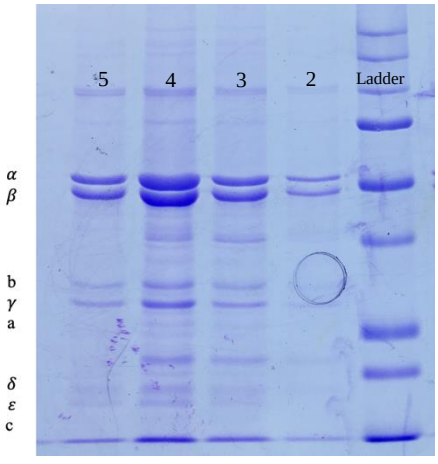

Figure 2: SDS-Page gel showing bands where subunits are seen. Fractions 2-5 are elution fractions.

aliquots. These are separated using SDS-Page gel electrophoresis. The aliquots showing all subunits present (Figure 2) are pooled and concentrated down *via* centrifugation.

A Lowry assay utilizing a BSA standard is conducted in order to determine the concentration of protein present, typically a concentration of 5 mg/mL are obtained. The protein is then spin-labelled using MTSL at a 40:1 ratio of MTSL to cysteine. For aM93C mutants a 10:1 ratio is used since methionine 93 protrudes outside the membrane. Half of the spin label is added, and it is allowed to incubate at room temperature for 2 hours before the remaining MTSL is added, where the protein is transferred to ice overnight. The protein is then further purified using FPLC in order to remove any free spin before spectra are collected.

2.2. EPR

Spin-labeled protein (30-50 uL) is loaded into a 50 uL capillary tube which is then sealed with wax and wiped clean. While the instrument is in standby mode the sample is added. The EPR is them switched to TUNE mode and the instrument is allowed to calibrate. The instrument is set to 5mW microwave power with a modulation amplitude of 1.2 G. Approximately ~25 x 90 s scans are collected and averaged for final spectra. EPR samples are typically run with ADP and ATP, as well as at pH 5 and 8. This ensures that it is running in the hydrolysis and synthesis direction for more complete data.

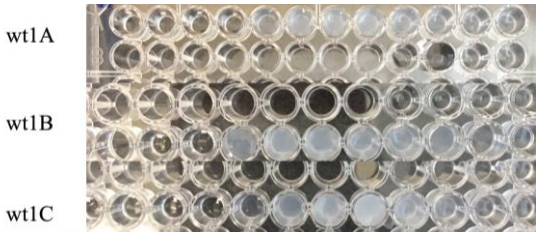

Figure 3: Post G-50 column aliquots where the turbid fractions represent proteolipids.

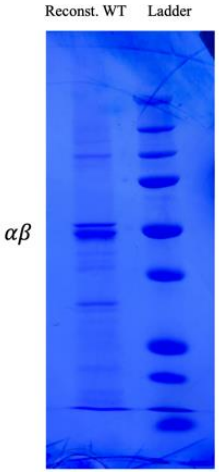

Figure 4: SDS-Page Gel of phosphatidylcholine proteolipids from concentrated G-50 aliquots. Gel indicates presence of all subunits.

2.3. Reconstitution

For reconstitution lipids must be prepared. Phosphatidylcholine (0.03 g) is dissolved into 1 mL of chloroform. The chloroform is evaporated under dry N_2 and resuspended in 3 mL Buffer A (10 mM Tricine KOH, pH 8, 2.5 mM $MgSO_4$, 0.1 mM Na_2EDTA, 0.5 mM DTT), taking care to keep lipids moisture free until buffer is added should be white and opaque. The lipid suspension undergoes 5 freeze-thaw cycles in liquid N_2 and us run through the extruder 10 times. The lipids should appear more transparent. Vesicles should be unilamellar after homogenization. In triplicate; 500 uL of 30mg/mL unilamellar vesicles are combined with 60 uL of 1% Sodium Cholate and 40 uL of ~5 mg/mL, and the proteolipids are separated utilizing exclusion chromatography.

A column volume of Buffer A is run through of beads before the 600 uL lipid suspension is added to the column. Aliquot in 300 uL 96-well plate adding Buffer A to the column as needed in 1mL increments until 4 mL, this is done in triplicate. There should be turbid fractions for each sample (Figure 3) these are pooled and pelleted. The pellets are resuspended, and an SDS-Page gel (Figure 4) and Lowry assay are conducted to verify proteins presence and concentration. Reconstitution was also conducted with *E. coli* lipid extract. 75 mg of *E. coli* lipid extract is combined with 25 mg of phosphatidylcholine and reconstitution is conducted as outlined about. Functionality is to be verified utilizing fluorescence assay.

2.4. SMA Extraction

Extraction screening was conducted on several polymers at a concentration of 2% (Figure 5) where SMA 300105 was found to be most effective at protein extraction due to prominent $\alpha\beta$ bands. SMA extraction is conducted with variations of the extraction and elution buffers used in the DDM extraction, Labeled Ni-A (50 mM Tris-HCl, 5 mM $MgCl_2$, 10% v/v glycerol, 2 mM imidazole, 40 mM caproic acid, 15 mM 4-amino benzamidine, pH 8) and Ni-B (50 mM Tris-HCl, 5 mM $MgCl_2$, 10% v/v glycerol, 200 mM imidazole, 40 mM caproic acid, 15 mM 4-amino benzamidine, pH 8). SMA is added to vesicles to an amount of 2% (v/v) dropwise at room temperature with stirring and allowed to incubate for 1 hour. The suspension is then then pelleted, and the supernatant is equilibrated with the Ni beads. The column is run utilizing the Ni-A and Ni-B buffers and the fractions are run on a SDS page gel and stained with Coomassie.

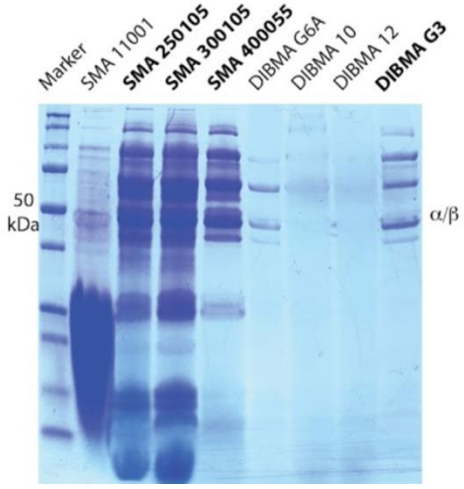

Figure 5: Lipid nano particle screening kit SDS-Page gel. Gel indicates SMA has much better extraction than DIBMA polymers. SMA 300105 show most prominent bands.

3. Results and Discussion

EPR data was collected for aM93C with 5 mM ATP, 5 mM ADP and at pH 5 and pH 8 respectively (Figure 6). The difference in lines of the ADP and ATP suggests that the 93 position has expected high backbone mobility. The pH spectra revealed little more about the position, no major conformational changes are indicated by the spectra.

This is what was anticipated due to methionine 93 protruding outside the membrane. These spectra correspond to the first peak from the FPLC which was later verified to be a high mass contaminate by gel electrophoresis (Figure 6). The majority of protein was found to be in the second peak of the FPLC raising the question of what the contaminant is. This contaminant is expected to be an aggregate or dimer due to its high mass. Presence of Histidine on the contaminant could potentially compromise structural results obtained by EPR. Additionally, the second peak will be analyzed in future experiments. Reacting the mutant with MTSL resulted in EPR spectra with too much noise to interpret. This is likely due to free spin label as Methionine 93 is thought to protrude from the membrane. When a smaller ratio of MTSL is added the spectral line becomes readable.

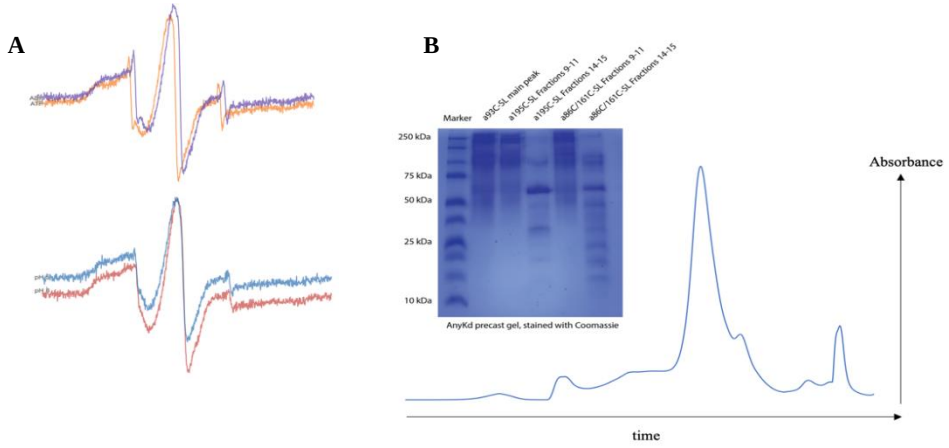

Figure 6: **A**: EPR spectra of main peak indicating residue mobility of contaminant. **B**: FPLC elution curve and corresponding SDS-Page Gel with peaks labelled. Characteristic bands are seen eluting in fractions 14-15.

EPR of proteolipids revealed no signal due to low protein concentrations. Higher concentrations (~1.2 mg/mL) proteolipids were successfully isolated, however, assays utilizing fluorescent quenching of ACMA yielded no functionality (Figure 7). This could be due to the spontaneous formation of multilamellar vesicles or the decoupling of F_1 and F_o motors. More work must be done to troubleshoot vesicles. Vesicles are particularly hard to work with and much troubleshooting is required in order to determine the state of the vesicles. Utilizing SMALPs is an easier protocol

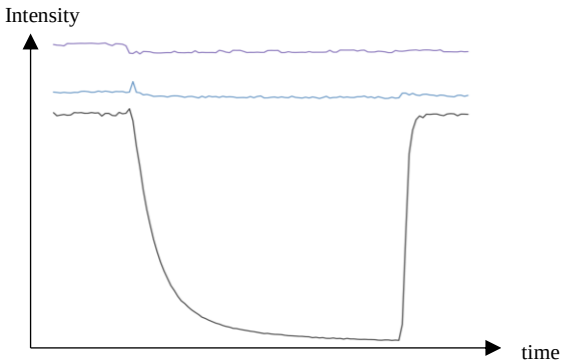

Figure 7: Proton pumping data. Black ISO WT, Blue *E. coli* lipid extract, Purple phosphatidylcholine. These data indicate that proteolipids are nonfunctional.

with a natural composition making it more favorable than reconstitution. While screening with SMALPS and DIBMA yielded the characteristic αβ hexamer in the SDS page gels (Figure 5), a successful Ni bead column has only been moderately successful with only faint bands visible (Figure 8). Visualizing the binding flow-through by SDS-Page, it is evident that the protein is not binding to the beads. This could be due to lower than usual salt concentrations in the Ni-A and Ni-B buffers. SMALPs also restricts the ability to create a proton gradient, prompting the development of different methods to determine functionality. A low pH stable SMA is also needed in order to collect EPR spectra for the synthesis direction. Additionally, the affinity chromatography can be conducted on a cobalt column which has a higher affinity with His tags.

With functional proteolipids, EPR spectra can be collected on proteins in an environment more akin to their native membrane. This would bolster the data reliability, and all mutants can be tested in their non-soluble environment. The experiment can be pursued further by the introduction of cardiolipin into the proteolipids. With the use of SMA protein can be extracted and analyzed in their native membrane environments in a protocol much easier and more reproducible than reconstitution. Comparing spectra of soluble protein to membrane embedded protein can reveal information regarding the potential roles the lipid environment is playing in the F_o mechanism.

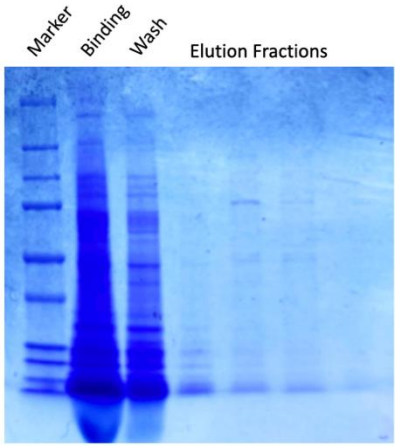

Figure 8: Post affinity SDS-Page SMA 300105 extraction.

4. Conclusion

Data obtained from the EPR spectra of the aM93C mutant is consistent with that of an exposed spin label. Additionally, no response to protonation or nucleotide binding was observed. Spectra must be collected free of the contaminant. Formation of proteolipids have been confirmed by Lowry assay, but functional assays still yield no results. Further optimization will feature implementation of different natured functional assays in order to diagnose the problem. Additionally, some of the previously attempted procedures for reconstitution may be revisited and conducted with the extruder. Different detergents could play a role in the negative results so alterative detergents may be tested, and a different detergent extraction method may be implemented in purification. Obtaining a procedure for reconstitution of ATPase could offer valuable insight to the work done in the Steed lab. Development of a protocol for SMA extraction would not only be a quicker purification method but would provide data on the functionality of ATPase in its native lipid environment. This would prompt research into the characterization of the lipid profile around the F_o subunit utilizing mass spectroscopy.

5. References

1 Sobti M, Smits C, Wong A. S. W., Ishmukhametov R, Stock D, Sandin S, Stewart A. G. (2016) Cryo-EM structures of the autoinhibited E. coli ATP synthase in three rotational states. *ELife*

2 Fillingame R. H., Steed P. R., (2014) Half channels mediating H+transport and the mechanism of gating in the Fosector of Escherichia coli F1FoATP synthase. *Biochimica et Biophysica Acta - Bioenergetics*. Elsevier.

3 Kühlbrandt W, Davies K. M. (2016, January 1) Rotary ATPases: A New Twist to an Ancient Machine. *Trends in Biochemical Sciences*. Elsevier Ltd.

4 Hiroyuki N., Ryohei Y., Masasuke Y., Kazuhiku K. (1997, March 20) Direct Observatiob of the rotation of F1-ATPase: *Nature* 386

5 Steed P., Fillingame R., (2009, June 18) Aqueous Accessibility to Transmembrane Regions of Subunit *c* of the *Escherichia coli* F1Fo ATP Synthase: *Journal of Biological Chemistry, 284*(35) 23243-23249

6 Mühleip, A., McComas, S. E., Amunts, A. (2019). Structure of a mitochondrial ATP synthase with bound native cardiolipin. *ELife, 8*.

7 Spikes, T. E., Montgomery, M. G.,Walker, J. E. (2020). Structure of the dimeric ATP synthase from bovine mitochondria. *Proceedings of the National Academy of Sciences*, 202013998.
8 Sobti, M., Walshe, J. L., Wu, D., Ishmukhametov, R., Zeng, Y. C., Robinson, C. V., … Stewart, A. G. (2020). Cryo-EM structures provide insight into how E. coli F1Fo ATP synthase accommodates symmetry mismatch. *Nature Communications, 11*(1).

9 Han, C. T., Song, J., Chan, T., Pruett, C., & Han, S. (2020). Electrostatic Environment of Proteorhodopsin Affects the pKa of Its Buried Primary Proton Acceptor. *Biophysical Journal*, *118*(8), 1838–1849.

10 Wang, L., Tonggu, L. Membrane protein reconstitution for functional and structural studies. *Sci. China Life Sci.* **58,** 66–74 (2015).

11 Miller J. H., Rajapakshe K. I., Infante H. L., Claycomb J. R. (2013) Electric Field Driven Torque in ATP Synthase. *PLoS ONE*, 8(9)

12 Xing, J., Wang, H., Von Ballmoos, C., Dimroth, P., & Oster, G. (2004). Torque generation by the Fo motor of the sodium ATPase. *Biophysical Journal*, *87*(4), 2148–2163.

13 Kubo, S., Niina, T., & Takada, S. (2019). Molecular dynamics simulation of proton-transfer coupled rotations in ATP synthase F O motor. *BioRxiv*, 618504.

14 Altenbach C, Greenhalgh A. D., Khorana H. G., Hubbell L. W. (1994) A collision gradient method to determine the immersion depth of nitroxides in lipid bilayers: Application to spin-labeled mutants of bacteriorhodopsin. Biophysics 94(1667-1671)

15 Zhang Y., Fillingame R. (1994, February 18)Essential Aspartate in Subunit *c* of F1Fo ATP Synthase: *The Journal of Biological Chemistry, 269*(7) 5473-5479

16 Hubbell W. L., Cafiso D. S., Altenbach C. (2000) Identifying conformational changes with site-directed spin labeling. *Nature Structural Biology*.

17 Kurian, P.; Capolupo, A.; Craddock, T. J. A.; Vitiello, G. Water-mediated
correlations in DNA-enzyme interactions. 2017. DOI: https://doi.org/10.1016/j.physleta.2017.10.038

6. Appendix

6.1. Mechanical Modeling

6.1.1. motivation

Physically modeling the motion of ATP synthase is difficult as you must resort to continuum models. Computational studies simplify this fact by first obtaining free energy profiles of the system. Solving the PBE provides insight on the electrostatics but results in incredibly complicated models involving nonlinear stochastic PDEs. These models provide insight into the energetics and possible electrostatic mechanisms but are convoluted and offer little intuition to the physics at work. There are too many charges at play to consider every point charge in the system. This motivates the Development of a mechanical model that describes the motion of the whole F_1F_o ATPase system. This mechanical model rejects the notion of the Brownian Rachet assuming that, while Brownian motion is at play, the thermal fluctuations are not sufficient to overcome the partition energy threshold (the 10 binding sites in the *c*-ring). While a mechanical model is a theoretical approach with few ties to experimental data, it can offer mechanical mechanisms that would be required to obtained to observed motion, particularly the mismatch in frequencies.

6.1.2. oscillator model

In order to make a comprehensive mechanical model assumptions must be made to simplify the system (Figure 1A). Since ATP synthase functions *via* rotations, that motion is a good starting point. Rotation of the *c* subunit is the basis for the oscillator model, where F_o is a harmonic oscillator with equations of motion

$$m_0\ddot{x} - b\dot{x} + k_0 x = f(t) \tag{1}$$

where *b* represents a damping coefficient, k_0 represents the spring constant of F_o and $f(t)$ is an arbitrary driving force that represents the pmf. Here the effect of Brownian motion is not considered. This yields a solution of the form $e^{i\omega t}$ which is a sinusoidal solution that describes the rotation of F_o in the complex plane. The influence of Brownian motion can be obtained by later adding a noise term $\eta(t)$ turning the equations of motion into a modified Langevin equation. Since the pmf is the combination of chemical and electric potential the impulse response can be used to obtain the transfer function of the system. Assuming a stochastic input such as an exponentially decaying or sigmoidal driving force, Green's functions can be used to solve the equations of motion.

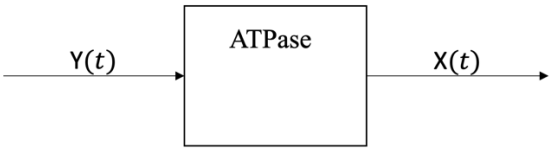

Figure 1A: Controls model where Y(t) is the input and X(t) is the output

Now considering the whole F_1F_o system, which can be described by coupling the F_o oscillator to an oscillator representing F_1 (Figure 2A). Here the equations of motion are derived from the Lagrangian with no damping constraints for simplicity. Here the spring with spring constant k_1 represents the γ stalk. The masses M_1 and M_0 oscillate at different frequencies according to the undamped solution which demonstrates how the springlike behavior of γ can compensate for the symmetry mismatch (Figure 3A). This can be generalized by summing together the two solutions and defining the symmetry mismatch as a function of phase and group velocity of the resulting beat frequencies.

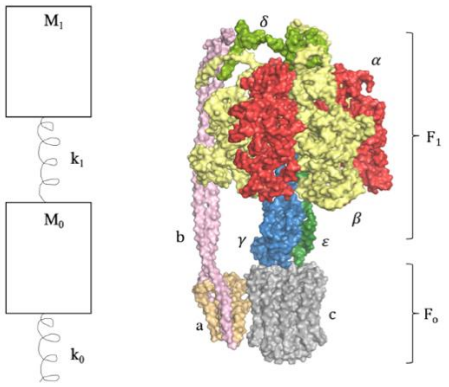

Figure 2A: Coupled oscillator model

6.1.3. limitations

The major limitation of the oscillator model includes the disregard for the electrostatics, the simplification of the system and the lack of experimental evidence regarding the mechanics. The next steps in the model would be to implement constraints to the coupled masses and treat it as a nonholonomic system. The solution for this will be more difficult to obtain but will be closer to approximating parameters for the spring constants and the magnitude and nature of the driving force.

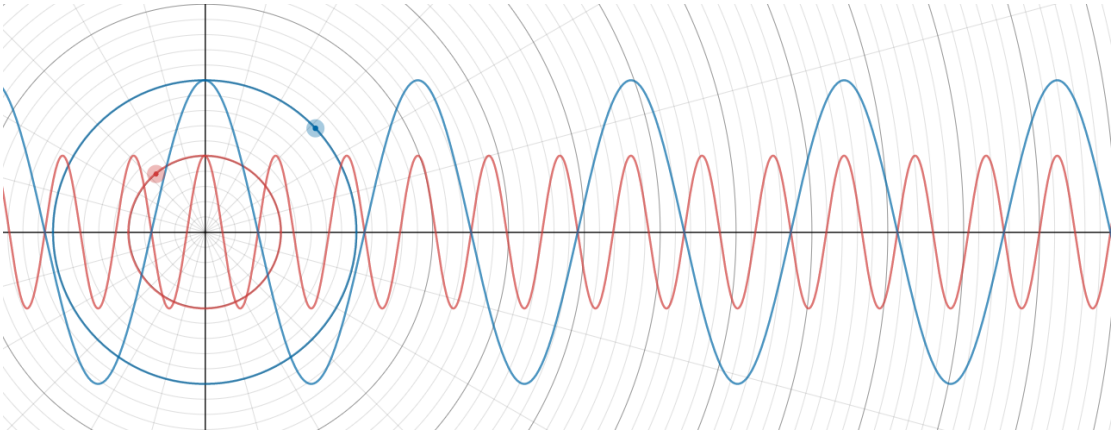

Figure 3A: Solution to coupled oscillator plotted with different amplitudes. Red is F_o and Blue is F_1

6.2. Quantum Field Theory Models

In recent years quantum field theory (QFT) has been proposed as a method to better understand protein structure and dynamics as a function of spontaneous symmetry breaking.[17] While these studies are theoretical, they do demonstrate how the theory can be used to predict macro behavior of a large, effectively N-body, system. Applying QFT to ATP synthase could describe the start-stop mechanism as a violation of certain group symmetries required for the motors to operate.

6.3. Transport and Electrostatic Models

Another interesting option is to consider the charge distribution as a function of a diffusion process (representing our pmf once again). This involves describing voltage as a function of charge distribution by the PBE, which is then coupled to a diffusion process. These two coupled PDEs are easy to interpret but defining the boundary conditions around the membrane on the N and P side would require more extensive research in the electrodynamics at play. Additionally, a special case of the PBE is required that implies that the charge distribution is also a function of voltage which complicates the means by which the PDEs are coupled.